

Insights into Platinum Complex-HSA Bindings: Spectral and Molecular Dynamics Simulation Studies

A. Ashrafi^a, M.M. Alavianmehr^a, D. Mohammad-Aghaie^{a*}, R. Yousefi^b, M. Golbon Haghghi^c, A.A. Moosavi-Movahedi^d and M.N. Soltani Rad^a

^aDepartment of Chemistry, Shiraz University of Technology, Shiraz 71555-313, Iran

^bProtein Chemistry Laboratory (PCL), Department of Biology, Shiraz University, Shiraz 71454, Iran

^cDepartment of Chemistry, Shahid Beheshti University, Evin, Tehran 19839-69411, Iran

^dInstitute of Biochemistry and Biophysics (IBB), University of Tehran, Tehran, Iran

(Received 13 October 2020, Accepted 21 March 2021)

Mutual interactions of human serum albumin (HSA) with the two binuclear platinum complexes, containing [Pt₂Cl₂(bhq)₂(μ-dppm)] (1) and [(*p*-MeC₆H₄)(bhq)Pt(μ-dppm)Pt(bhq)(CF₃CO₂)] (2), in which bhq = benzo[h]quinoline, and dppm = bis(diphenylphosphino) methane, were thoroughly investigated using spectroscopic and molecular modeling techniques. In this respect, fluorescence, Ultraviolet-visible (UV-Vis) and circular dichroism (CD) spectroscopies, along with the docking and molecular dynamics simulations (MD) were utilized. Analysis of spectroscopic and MD simulation results revealed the structural alterations of HSA upon binding to the binuclear platinum complexes, while the hydrogen bonding and van der Waals forces were found to mainly contribute to the protein-ligand intermolecular interactions. Results of far-UV CD measurements showed the strong ability of platinum complexes in reducing the α-helical content of HSA, while increasing the other secondary structural features. Due to their different chemical natures, these complexes bind to HSA in different manners. Binding constants and thermodynamic binding parameters between these complexes and HSA were calculated using the Stern-Volmer and van't Hoff equations. Calculated thermodynamic binding parameters indicated that the interaction is spontaneous and enthalpy driven, through the static and dynamic quenching mechanisms, for complexes 1 and 2, respectively.

Keywords: Protein-ligand interaction, HSA, Platinum complex, Fluorescence spectroscopy, Molecular dynamics simulation

INTRODUCTION

The metal coordination compounds have gained considerable interest because of their biological properties and anticancer activities [1]. These compounds are widely used in the treatment of several cancer types and human tumors. Application of metal-based drugs depends on their effects in inducing DNA damages and their ability to detect target cells [2]. Researchers have recently focused on the design of novel anticancer platinum complexes with improved pharmacological properties, such as selective detection of cancer cells and reduced level of side effects

[3].

Human serum albumin (HSA) is the most well-characterized serum protein (30-50 g l⁻¹) in blood plasma that contains 585 residues, consisting of three domains (I, II and III) [4]. It has various biological functions including ability to retain the pH and osmotic pressure of blood. Also, this protein possesses an outstanding role in transport of a wide variety of endogenous and exogenous ligands [5]. This carrier protein of bloodstream also plays a significant role in interaction with various drugs to improve their delivery and facilitate the process of drug access into its target cell [6].

Recently, Chaves *et al.* [7] investigated the binding of two porphyrin-based tetra-cationic photosensitizers, 4-MeTPyP and 4-PtTPyP, to HSA, using spectroscopic

*Corresponding author. E-mail: d_ghaie@sutech.ac.ir

techniques and molecular docking simulation. In the case of 4-MeTPyP, binding to HSA was found to be mainly enthalpy driven, while for the other compound, 4-PtTPyP, binding occurred due to the hydrophobic forces in an entropy driven association. The results of far UV CD indicated that 4-PtTPyP perturbs the thermal stability of the protein, owing to the high volume of porphyrin.

Shahabadi *et al.* [8] studied the interaction of a new platinum(IV) complex with HSA using the UV-Vis, fluorometric and circular dichroism (CD) spectroscopies, and the molecular docking method. Hydrogen bonds and van der Waals interactions were the main forces, contributing to the stability of the HSA-Pt(IV) complex, while the static quenching mechanism was responsible for the fluorescence quenching of HSA. Analysis of CD and UV-Vis spectroscopies revealed the structural changes in HSA due to binding with this complex.

In 2019, Yasrebi *et al.* [9] studied the interaction of HSA with the six related uranyl complexes of alkyl substituted isothiosemicarbazone, both experimentally and theoretically. UV-Vis, fluorescence and circular dichroism spectroscopies were utilized as the probes to determine the effect of alkyl group chain length on the strength and nature of the HSA-ligand interaction. Obtained results showed that the studied ligands quench the fluorescence emission of HSA significantly and cause unfolding the polypeptide of HSA through converting the α -helical content to β -structures and random coil. Interestingly, it was found that the length of alkyl chain group does not have a significant impact on the HSA-ligand interaction.

Considering the importance of anticancer platinum complexes, studies on their binding to HSA can provide useful information which can be employed in biomedical and pharmaceutical sciences [10]. In this study, the binding of two binuclear platinum complexes with HSA was explored using UV-Vis, fluorescence and circular dichroism spectroscopies along with docking analysis and molecular dynamics simulation. Stern-Volmer and van't Hoff equations were used to determine the binding constants and thermodynamic binding parameters between these complexes and HSA. Moreover, molecular docking and molecular dynamics simulation (MDS) were utilized to identify the platinum complexes' binding sites on HSA.

MATERIALS AND METHODS

Materials

HSA, all materials and reagents were purchased from Sigma-Aldrich Company with the analytical grade. The HSA solution was prepared by dissolving HSA in 50 mM Tris-HCl buffer pH 7.4 containing 10 mM NaCl (TN buffer). HSA concentration was determined spectrophotometrically through using a molar extinction coefficient of $36,000 \text{ M}^{-1} \text{ cm}^{-1}$ at 280 nm [11].

Methods

Synthesis of the binuclear Pt(II) complexes. The binuclear platinum complexes were synthesized following the procedure reported in the previously published works [12,13].

Spectral Measurements

UV-Vis absorption experiment. The UV-Vis absorption measurements were performed in TN buffer by using a fixed concentration of HSA at $10 \mu\text{M}$ while varying the concentrations of the platinum complexes from 0 to $18 \mu\text{M}$. The absorption spectra were recorded using a CE 7200 UV-Vis spectrophotometer instrument (Cecil Instruments Ltd., UK) after incubation of the samples for 5 min in the presence of the binuclear platinum complexes 1 and 2, in the range of 230-450 nm at 298 K.

Intrinsic Fluorescence Measurements

The fluorescence spectra of HSA were recorded at 288, 303 and 310 K with a Carry-Eclipse spectrofluorometer (Model Varian, Australia) equipped with an automatic temperature controller. The fluorescence emission titration experiments were performed using a fixed concentration of HSA ($3 \mu\text{M}$) with various concentrations of the platinum complexes (0-18 μM). The emission spectra of HSA in the presence of increasing concentrations of each binuclear platinum complex were recorded between 300-450 nm, at an excitation wavelength of 295 nm.

The synchronous fluorescence spectra of HSA ($3 \mu\text{M}$), in the presence of various concentrations of binuclear platinum complexes (0-18 μM), were also obtained ($\Delta\lambda = 15 \text{ nm}$ and $\Delta\lambda = 60 \text{ nm}$). The slit widths were fixed to 5 and 10 nm for excitation and emission, respectively [14].

The Competitive Binding Assay

HSA contains two main binding sites I and II for various ligands that can be illustrated by two specific site markers, warfarin and ibuprofen, respectively [15,16]. These site markers have been previously used to investigate the binding site and also competitive binding analyses of the platinum complexes on HSA. The competitive binding measurements were recorded by using a fixed concentration of HSA and warfarin/ibuprofen at 3 μM with various concentrations of the platinum complexes (0-15 μM). The emission spectra of HSA-warfarin/ibuprofen in the presence of increasing concentrations of each binuclear platinum complex were recorded between 300-500 nm, at an excitation wavelength of 295 nm.

Protein Surface Hydrophobicity Assessment

8-Anilinoanthracene-1-sulfonic acid (ANS) is an organic compound, containing both sulfonic acid and an amine group, which is used as a fluorescent molecular probe. The ANS binding analysis was used to explore the hydrophobicity of studied platinum complexes upon interaction with HSA. Fixed concentrations of HSA (3 μM) and ANS (200 μM) were incubated for 20 min at 25 °C under dark condition. The emission intensities of HSA-ANS in the presence of increasing concentrations of each binuclear platinum complex (0-18 μM) were recorded between 400-600 nm after 5 min excitation of ANS at 365 nm [17].

The Circular Dichroism Experiment

The CD measurements of each binuclear platinum complex with HSA were recorded in TN buffer at 25 °C with a JASCO (J-810) spectropolarimeter. The CD spectra were carried out by keeping constant the HSA concentration at 9 μM while varying concentrations of the platinum complexes (0, 5, 10 and 20 μM). Each sample was scanned in a wavelength range between 190 and 260 nm using a 1 mm path length cuvette. The data were expressed as a molar residue ellipticity [0] [18]. The CDNN secondary structure analysis software was used to predict the secondary structure content of the HSA protein [19].

Molecular Dynamics (MD) Simulation

Initial structure of HSA with PDB entry code 1BM0

[20], composed of two identical chains A and B, was taken from the protein data bank. Only chain A of HSA was subjected to the molecular dynamics simulation, using the GROMACS 4.5.5 simulation package [21-23]. The `pdb2gmx` command was employed to extract the interaction parameters of HSA, based on the GROMOS96-53a6 force field [24]. The protein molecule was placed in a cubic box, containing 43624 simple point charge (SPC) water molecules [25]. Due to the 15 negative charges on HSA, fifteen Na^+ counter ions were added to neutralize the whole system.

First, the energy minimization (EM) was carried out on the system, using the steepest descent method for 1ns, with the cut off value of 1.4 nm, for van der Waals and Coulomb forces. EM ensured having a reasonable starting structure, in terms of geometry and solvent orientation.

In the two following NVT and NPT equilibration steps, the protein backbone was fixed and position-restrained for 1 ns, letting the solvent and counter ions to equilibrate around the protein. Finally, the whole system was subjected to 20 ns real molecular dynamics simulation, at 310 K and 1 bar pressure (NPT ensemble).

Periodic boundary conditions were applied in all three dimensions, while the equations of motions were integrated using the leap-frog algorithm with a time step of 2 fs. Atomic coordinates were recorded in the trajectory file at every 1 ps during the simulation for further analyses.

The Molecular Docking Analysis

The energy minimization calculations of platinum complexes were carried out through the density functional theory (DFT), at the B3LYP computational level. The chosen basis sets for Pt and all other atoms (Fig. 1) were respectively LanL2DZ and 6-31G, implemented in Gaussian 09 [26].

The energy minimized platinum complexes and the simulated HSA protein were both imported to the Molegro Virtual Docker (MVD)[27] workspace, in order to carry out the protein-ligand docking.

RESULTS AND DISCUSSION

The UV-Vis Absorption Analysis

The binding of binuclear platinum complex with HSA

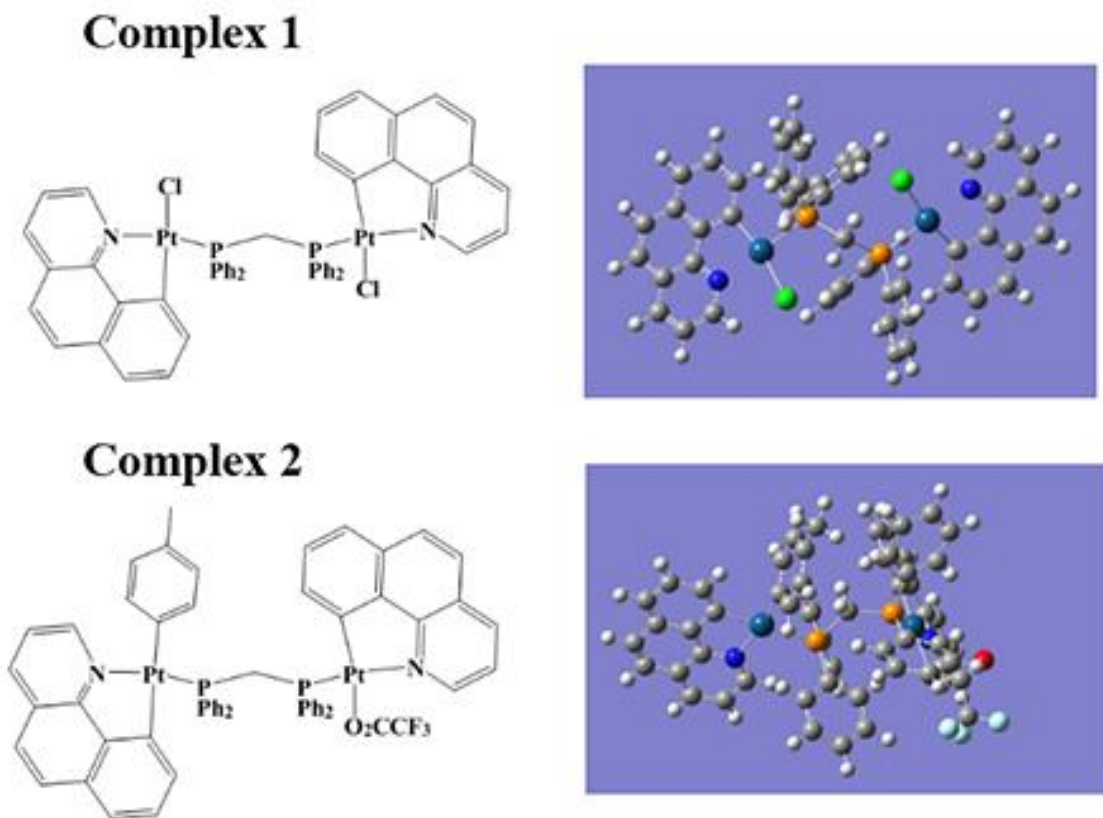


Fig. 1. The chemical and optimized structures of binuclear platinum complexes.

is usually accompanied by the structural changes of the protein and its environment; therefore, UV-Vis absorption measurement is one of the most effective techniques to analyze the binding of metal complexes to HSA.

The spectra of HSA were recorded at 230–450 nm with a fixed concentration of HSA (10 μM) and gradual additions of the platinum complexes (0 to 18 μM). Observed enhancement in the UV-Vis absorption spectra of HSA at 250–300 nm (with the λ_{max} at 280 nm), in the presence of various concentrations of each binuclear platinum complex, can be attributed to the $\pi \rightarrow \pi^*$ transition of the aromatic amino acid residues, including tryptophan (Trp), tyrosine (Tyr) and phenylalanine (Phe) (Fig. 2) [28].

In fact, alterations in the intensity of HSA absorbance peak indicate that the micro environment around the aromatic amino acids of protein changes due to the interaction between HSA and platinum complexes.

Obviously, as the concentration of platinum complexes in the system increases, greater effect on the height of the absorption peak is observed.

Although there is no significant change in the maximum wavelength of HSA, after adding platinum complexes, the UV-Vis absorption spectra of HSA confirms the interactions of platinum complexes with this protein [29]. It is clearly seen that the complex 2 has greater effect on the absorption spectra of HSA.

Fluorescence Quenching Mechanism

Fluorescence spectroscopy can provide information on the protein (HSA) structural alterations upon binding to the platinum complexes [30]. Fluorescence quenching refers to any process able to decrease the fluorescence intensity of a given substance and requires molecular contact between the fluorophore and quencher. This contact can be due to

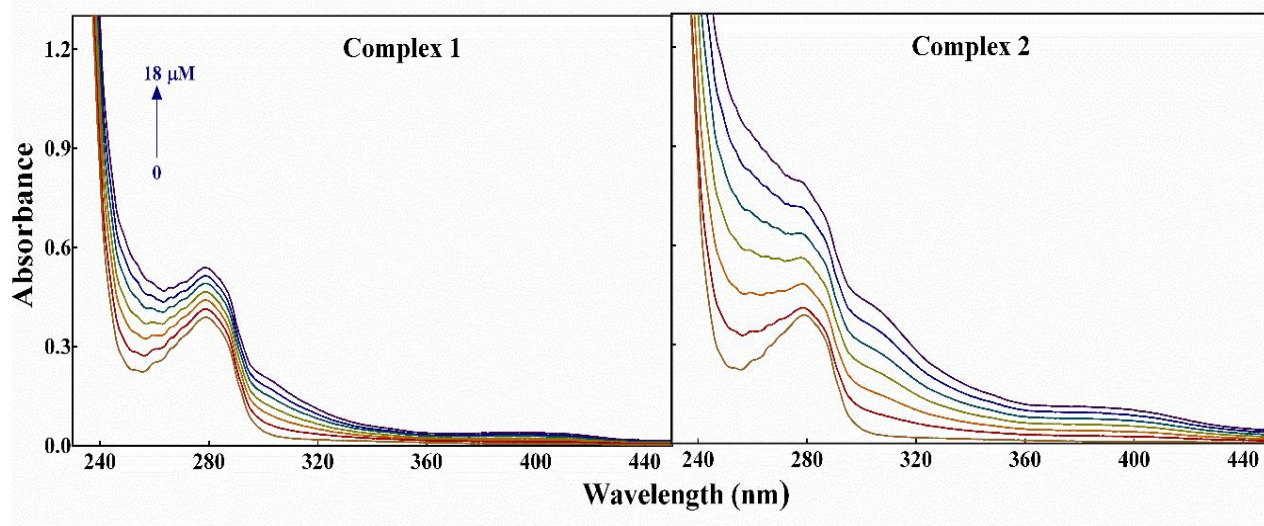


Fig. 2. The UV-Vis absorption spectra of HSA upon interaction with the two studied platinum complexes. HSA: 10 μM , Binuclear platinum complexes: 0-18 μM .

diffusive encounters or complex formation which are called dynamic and static quenching mechanisms, respectively. Based on their different dependence on temperature, dynamic and static quenching mechanisms can be distinguished. In the dynamic quenching, temperature increase causes the quenching rate constant to increase. This observation can be explained with the collisional encounters between the protein and quencher, resulting in the faster diffusion. On the other hand, in static quenching, temperature elevation results in reduction of the quenching rate constant. Decreased stability of the formed complex in higher temperatures is responsible for reducing the static quenching constant [31].

The fluorescence emission spectra of HSA were recorded at 288, 303 and 310 K in the presence of various concentrations of platinum complexes, in the wavelength range of 300-450 nm at excitation wavelength of 280 nm. Obtained spectra showed a gradual decrease in the fluorescence emission intensities of HSA with increasing concentrations of the platinum complexes, while no significant change was observed in the maximum emission wavelength of HSA (Fig. 3). This finding suggests that the changes in the microenvironment of HSA are attributed to the interaction with the platinum complexes. As explained

in the next section, the mechanism of HSA fluorescence quenching as well as thermodynamic binding parameters can be determined by using the temperature dependent of fluorescence emission experiment and the Stern-Volmer equation.

Determination of Quenching Mechanism

The mechanism of HSA fluorescence quenching can be determined by using the Stern-Volmer equation [14]:

$$F_0/F = 1 + K_q \tau_0 [Q] = 1 + K_{sv} [Q] \quad (1)$$

where F_0 and F are respectively the fluorescence intensities in the absence and presence of quencher (platinum complexes) and $[Q]$ stands for complex concentration. Moreover, K_{sv} is the Stern-Volmer quenching constant, and K_q and τ_0 correspondingly refer to the rate constant of quenching process and biomolecule average lifetime without a quencher ($\tau_0 = 10^{-8}$ s) [11].

In this study, the HSA fluorescence quenching was assessed in the presence of different concentrations of the platinum complexes, at various temperatures (288, 303 and 310 K), where the corresponding quenching parameters are listed in Table 1. The Stern-Volmer quenching constant in

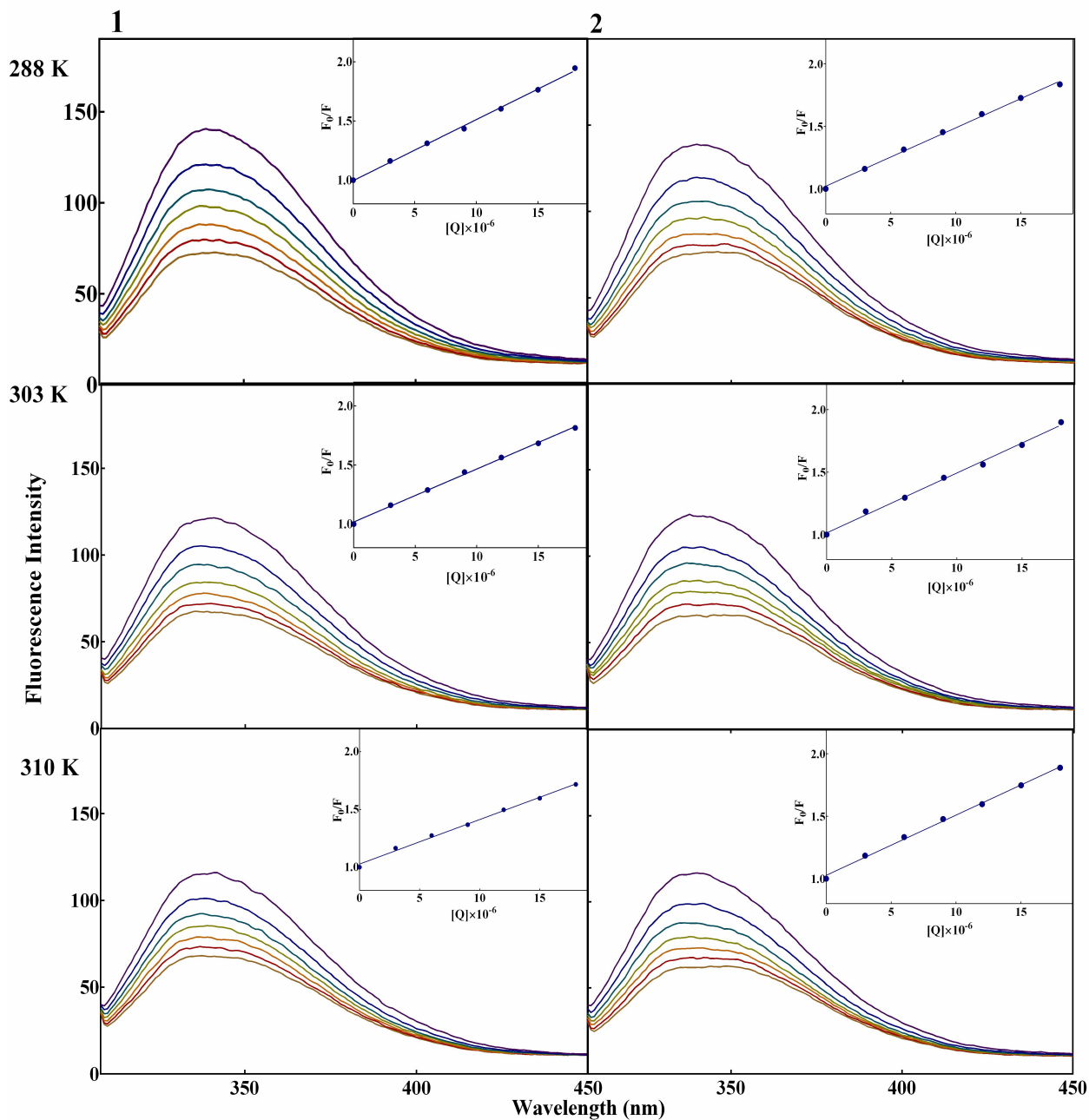


Fig. 3. Temperature-dependent fluorescence assessment of the interactions between the binuclear platinum complexes and HSA at 288 K, 303 K and 310 K. HSA: 3 μM , Binuclear platinum complexes: 0-18 μM .

complex 1 reduces with the temperature rise, indicating that the mechanism of HSA fluorescence quenching by this platinum complex could be static. The slight enhance of

HSA quenching rate constant with the temperature increase, in presence of complex 2, is an evidence for the dynamic quenching mechanism.

Table 1. Quenching Parameters of the Binding Platinum Complexes with HSA at Different Temperatures

Pt complex	T (K)	$K_{SV} \times 10^4$ (M^{-1})	$K_q \times 10^{12}$ ($M^{-1} s^{-1}$)	R^2
1	288	5.16 ± 0.001	5.16	0.997
	303	4.48 ± 0.001	4.48	0.998
	310	3.85 ± 0.001	3.85	0.995
2	288	4.67 ± 0.001	4.67	0.996
	303	4.79 ± 0.001	4.79	0.995
	310	4.83 ± 0.001	4.83	0.997

Calculation of Association Constant and Number of Binding Sites

When small molecules bind independently to a set of equivalent sites on a macromolecule, there will be an equilibrium between free and bound molecules governed by Eq. (1), in which K_b is the binding (association) constant to a site, and n is the number of binding sites per HSA molecule [32],

$$\log(F_0 - F/F) = \log K_b + n \log[Q] \quad (2)$$

where F_0 and F are the fluorescence intensities of HSA with and without the quencher (binuclear platinum complexes), respectively.

The modified Stern-Volmer plots were used to calculate the binding constant (K_b), and the number of binding sites (n) values at different temperatures (Fig. 4A). In this respect, slopes and intercepts of linear plots of $\log(F_0 - F/F)$ versus $\log[Q]$ were employed to obtain K_b and n values, respectively. Obtained results showed that the binding constants (K_b) are increased with the rising temperature, while complexes 1 and 2 demonstrated low and high affinities for HSA, respectively. The number of binding sites (n) is approximately unity for both synthetic platinum complexes at different temperatures, confirming the binding of each complex to one HSA molecule (Table 2).

The binding affinities of platinum complexes with HSA are in the range of 10^4 - $10^6 M^{-1}$, indicating that the effect of HSA on the pharmacokinetic properties of platinum complexes is in the same extents of some other drugs [33,34].

Thermodynamic Study of the Binding Process

The thermodynamic parameters at different temperatures can be determined from the van't Hoff equation [35]:

$$\ln K_b = -\Delta H/RT + \Delta S/R \quad (3)$$

$$\Delta G = -RT \ln K_b \quad (4)$$

where K_b is the binding constant at specified temperature T , and R is the universal gas constant. ΔH (enthalpy change) and ΔS (entropy change) values are calculated from the slope and intercept of the van't Hoff plot of $\ln K_b$ against $1/T$ at different temperatures, while ΔG is obtained through its direct relationship with $\ln K_b$ (Fig. 4B) [35].

Thermodynamic parameters are able to provide significant information on the type of dominant interaction forces [36]. For instance, the negative Gibbs free energy change (ΔG) illustrates the spontaneity of the interaction. On the other hand, negative ΔH and ΔS values in our

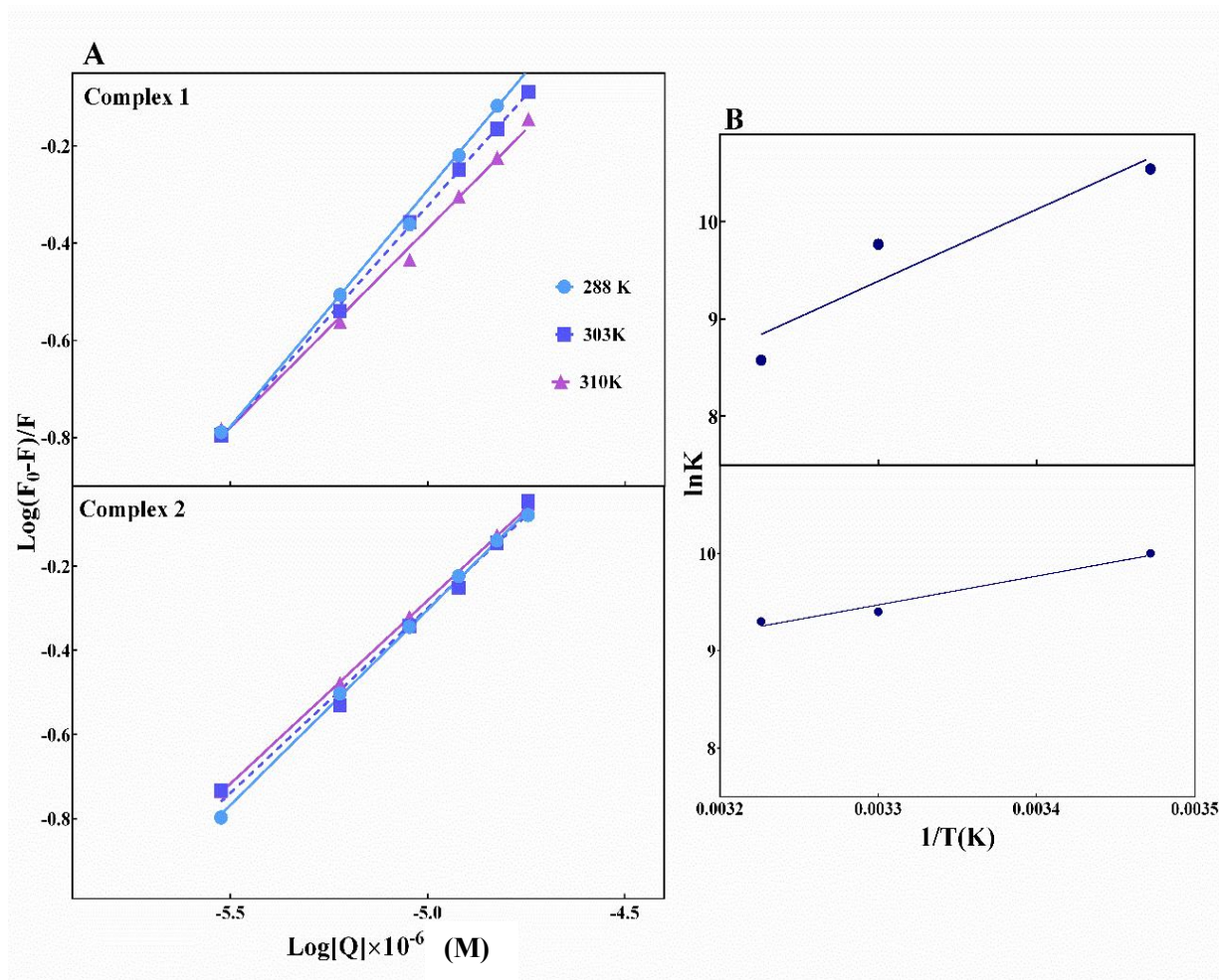


Fig. 4. A) The plot of $\log(F_0 - F/F)$ against $\log[Q]$ at three different temperatures (288, 303 and 310 K). B) The Van't Hoff plot obtained from bound HSA and platinum complexes.

studied complexes show that van der Waals interaction and hydrogen bonding are the main contributing forces in the interaction between HSA and the synthetic complexes (Table 3).

Synchronous Fluorescence Measurements

Intrinsic fluorescence of HSA is mainly derived from Tyr and Trp residues. In this study, the synchronous fluorescence (SF) of HSA was investigated to determine any changes in the microenvironments of Tyr and Trp residues as a result of binding to the platinum complexes. The fluorescence emission peaks of these aromatic residues

are sensitive to the polarity of their environment.

The excitation and emission monochromators were synchronously scanned, separated by a constant wavelength interval $\Delta\lambda$ ($\Delta\lambda = \lambda_{em} - \lambda_{ex}$). When $\Delta\lambda$ was set to 15 nm and 60 nm, the resulting SF spectrum, respectively, contained the characteristic features of Tyr and Trp residues in HSA. [37]. Figure 5 demonstrates the effect of adding platinum complexes on the synchronous fluorescence spectra of HSA, when $\Delta\lambda = 15$ nm (Fig. 5A) or $\Delta\lambda = 60$ nm (Fig. 5B).

Close inspection of this figure clearly shows that in both cases there is no notable Stokes shift at the maximum fluorescence emission after successive additions of platinum

Table 2. The Binding Constant (K_b), and Number of Binding Sites (n) for the Binding of Platinum Complexes to HSA at Different Temperatures

Pt complex (μM)	T (K)	$K_b \times 10^4$ (M^{-1})	n	R^2
1	288	3.79 ± 0.026	0.974	0.997
	303	1.75 ± 0.013	0.913	0.997
	310	0.53 ± 0.028	0.8191	0.995
2	288	2.21 ± 0.013	0.9282	0.999
	303	1.22 ± 0.044	0.8779	0.989
	310	1.11 ± 0.011	0.8716	0.997

Table 3. Thermodynamic Parameters of the Interaction of the Platinum Complexes with HSA

Pt complex (μM)	T (K)	ΔH (kJ mol^{-1})	ΔS ($\text{J K}^{-1} \text{mol}^{-1}$)	ΔG (kJ mol^{-1})
1	288			-25.25
	303	-81.4	-188.8	-24.61
	310			-22.11
2	288			-23.98
	303	-24.56	-2.321	-23.72
	310			-24.01

complexes to the HSA solution. This observation suggests the lack of significant change on the HSA structure upon ligand binding that can perturb the microenvironment around the Tyr and Trp residues.

It is noteworthy that the fluorescence intensity of Trp residues is considerably more intense compared to the Tyr residues. As mentioned before, the gradual decrement in the maximum absorption peaks of HSA with the increasing concentrations of platinum complexes is due to the

fluorescence quenching phenomenon.

The Competitive Displacement Analyses

As stated before, the binding domain of each platinum complex on HSA can be specified using warfarin and ibuprofen as characteristic markers for the sites I and II, respectively.

The fluorescence emission experiment was performed by addition of each platinum complex to the HSA-

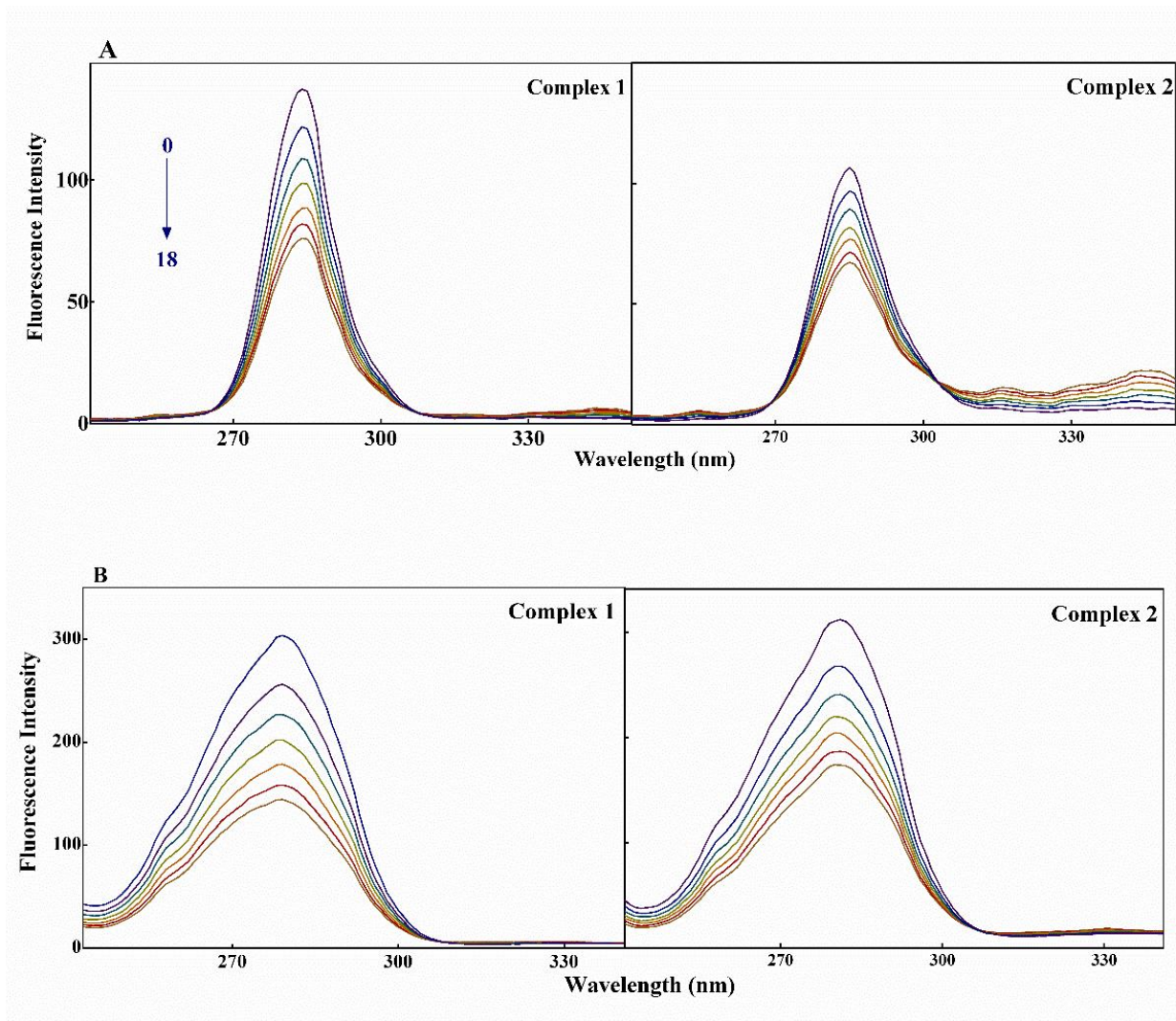


Fig. 5. The SF spectra of HSA due to adding different concentrations of platinum complexes for A) Tyr ($\Delta\lambda = 15$ nm), and for B) Trp ($\Delta\lambda = 60$ nm).

warfarin/ibuprofen solution at 298 K with the excitation wavelength fixed at 295 nm. As seen in Fig. 6, by adding warfarin to the HSA solution, the maximum emission peaks of the solutions demonstrated an obvious red shift, accompanied by the significant decrement in the fluorescence intensity. In contrast, there was no obvious difference with the addition of ibuprofen. Also, the reduction in the fluorescence emission spectra of HSA-warfarin/ibuprofen solution was observed in the presence of various concentrations of each binuclear platinum complex.

The quenching data were analyzed with the modified Stern-Volmer equation [38]:

$$\frac{F_0}{F_0 - F} = \frac{1}{f_a K_a} \frac{1}{[Q]} \quad (4)$$

here, K_a is the modified Stern-Volmer association constant for the accessible fluorophores, f_a is the fraction of accessible fluorescence, F_0 is the fluorescence intensity of HSA without the platinum complexes, and F is the

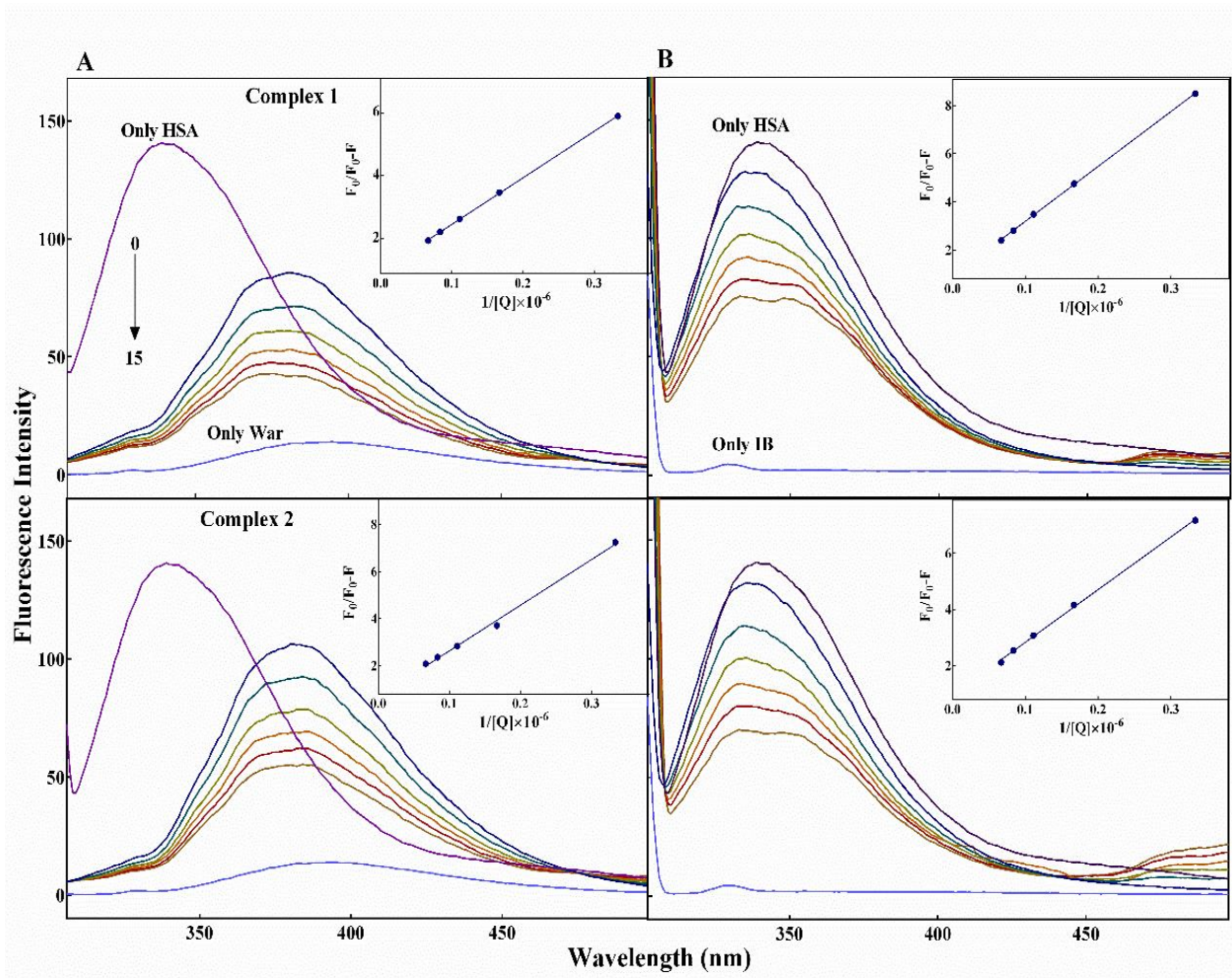


Fig. 6. Competitive displacement of warfarin (A) and ibuprofen (B) with the binuclear platinum complexes.

fluorescence intensity of HSA solution containing the platinum complexes with concentration $[Q]$ and site marker. Linear plots of $F_0/(F_0 - F)$ vs. $1/[Q]$ were employed to obtain the K_a and f_a values from the slope and intercept, respectively [17]. Equation (4) was used to explore the effect of platinum complexes on each site marker-HSA solution, and to obtain the corresponding association constant values reported in Table 4.

The results obtained show that the association constant of warfarin-HSA system in platinum complex 1 is relatively higher than that of ibuprofen-HSA system, so complex 1 displays higher affinity to locate in the region of site I on HSA. On the other hand, the association constant of

ibuprofen-HSA system in platinum complex 2 is nearly higher than that of warfarin-HSA system, suggesting that platinum complex 2 tends to displace ibuprofen from ibuprofen-HSA system which is located in site II on HSA.

The ANS Fluorescence Analysis

8-Anilino-naphthalene-1-sulfonic acid (ANS) is an organic compound containing both a sulfonic acid and an amine group that is used as a fluorescent molecular probe. This compound can be used to study conformational changes in proteins induced by ligand binding, as ANS's fluorescent properties will change when it binds to the hydrophobic regions on the protein surface. Comparison of

Table 4. The Association Constants of HSA-Warfarin/Ibuprofenin Binding with Binuclear Platinum Complexes

	K_a ($\times 10^5$ M ⁻¹)	
	Complex 1	Complex 2
HSA + W	0.665 ± 0.0153	0.352 ± 0.0125
HSA + I	0.405 ± 0.0295	0.516 ± 0.0619
R(W/I)	0.999/0.998	0.996/0.999

R: Correlation coefficient, W: warfarin, I: Ibuprofen.

the fluorescence in the presence and absence of a particular ligand can thus give information about how the binding of the ligand changes the protein's surface.

In this study, the ANS fluorescence analysis was utilized to assess the conformational changes of HSA upon interaction with platinum complexes. In fact, the ANS fluorescence analysis can provide information on the alteration of hydrophobic regions of HSA due to interaction with the platinum complexes [39]. Competition of platinum complexes with the bound ANS molecules to interact with the hydrophobic regions of HSA confirms the tendency of these complexes to establish interactions with the protein's hydrophobic regions.

As seen in Fig. 7A, the ANS fluorescence intensity of HSA shows gradual reduction in response to the increasing concentrations of platinum complexes. This observation confirms the separation of ANS molecules from the hydrophobic surface of HSA, which is then occupied by platinum complexes. In order to record these fluorescence emission spectra, constant concentrations of HSA and ANS molecules were incubated for 20 min in the dark, before adding various concentrations of platinum complexes.

On the other hand the two plots in Fig. 7B indicate that both platinum complexes have almost the same effect on the ANS fluorescence and the same potential to substitute the ANS molecules.

The Circular Dichroism Analysis

The UV-CD spectroscopy spectra is able to characterize

the secondary structural and conformational changes of protein, upon interaction with the platinum complexes [40]. As shown in Fig. 8, the far-UV CD spectra of HSA display two negative bands at 209 and 220 nm, that are characteristic of the right-handed α -helical structure contributed to the $n \rightarrow \pi^*$ transition in peptide bonds of α -helical structures of HSA [41].

The dominant secondary structural element of HSA is the α -helix (about 60%) along with a minor content of β -sheet structure [42]. The results of deconvolution of CD spectra indicated the significant reduction in the protein's α -helical content upon binding with platinum complexes, accompanied by the increase in quantity of β -sheet and β -turn secondary structures (Table 5). In total, the far-UV CD assessment of HSA suggests that binding of these complexes to HSA results in a considerable change in the secondary structure of this protein.

Molecular Dynamics and Docking Simulations

In order to computationally determine the binding domains of studied complexes on the HSA structure, optimized configurations of both protein and platinum complexes were needed. In this respect, the chain A of HSA molecule, extracted from the PDB code 1BM0, was simulated for 20 ns under almost physiological conditions using the Gromacs simulation package. Analysis of the root mean square deviation (RMSD) of the protein's backbone suggested that 20 ns of NPT simulation was sufficient for the protein structure to relax in the specified temperature

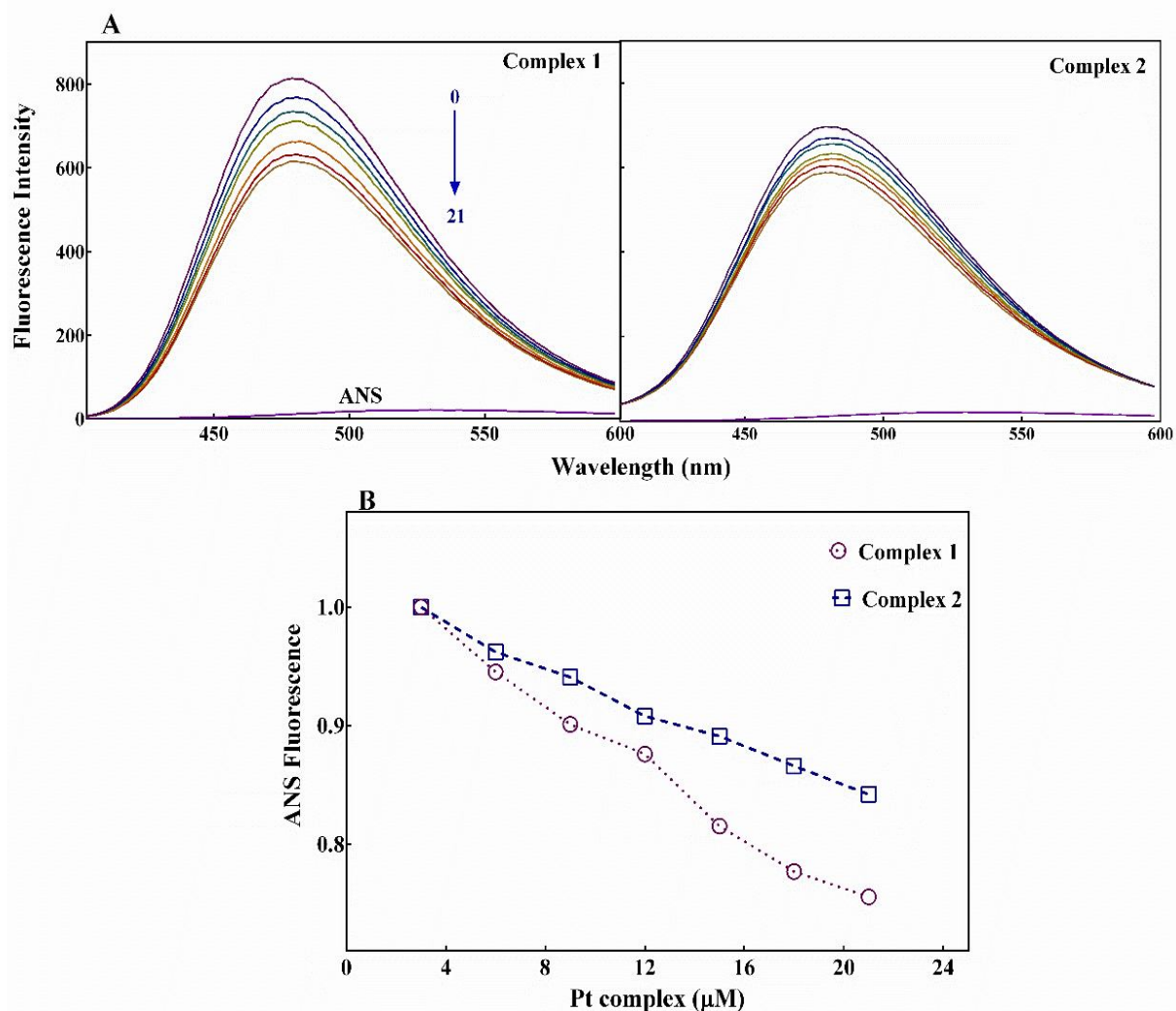


Fig. 7. A) The ANS fluorescence intensity of HSA in the presence of increasing concentrations of two platinum complexes. B) The maximum emission intensity of ANS vs. concentration of the synthetic platinum complexes.

and pressure conditions.

This quantity (RMSD) is usually employed to assess the stability of the studied structure. In fact, RMSD measures quantitatively the structural alterations of the protein's backbone through comparing two superimposed atomic coordinates from the two time points of the simulation trajectory.

As shown in Fig. 9, the RMSD backbone of free HSA at 310 K increases considerably in the first 2 ns, and fluctuates around the 0.3 nm value for the rest of the simulation time,

indicating that the protein's backbone is in its equilibrium state. This observation is satisfactory enough to employ the resulting HSA structure at the end of the 20 ns simulation time, as an optimized and appropriate configuration for the further determination of the binding domains of the platinum complexes on HSA.

On the other hand, the density functional theory (DFT) in the B3LYP computational level was carried out on the platinum complexes to obtain their energy minimized structures. Chosen basis sets for Pt and all other

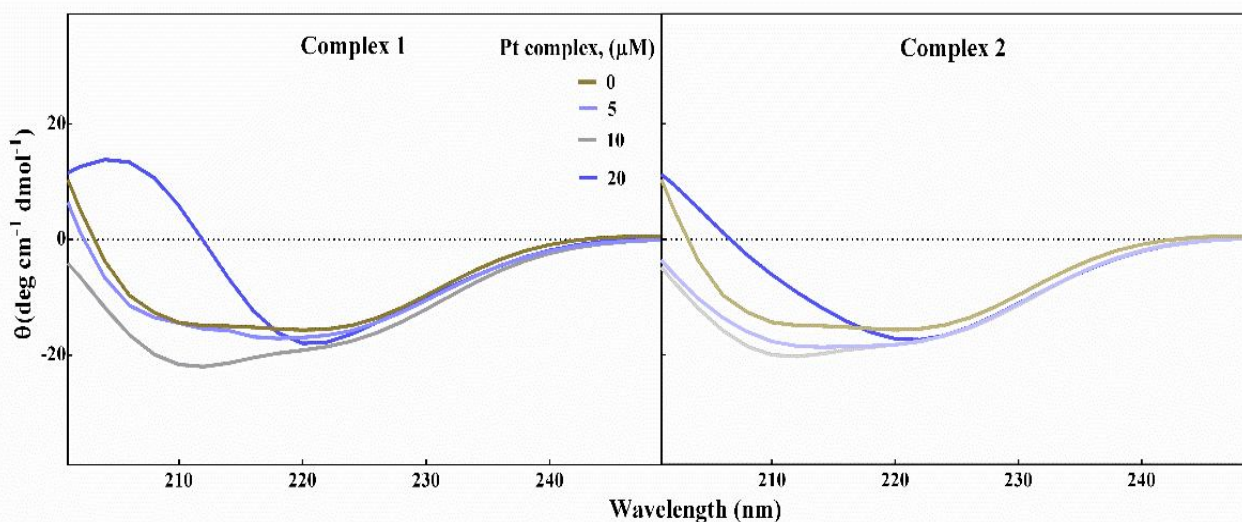


Fig. 8. Far-UV CD analysis of HSA in the presence of various concentrations of studied platinum complexes.

Table 5. Changes in the Secondary Structure of HSA upon Interaction with the Platinum Complexes

	Pt complex (μM)	α -helix (%)	β -sheet (%)	β -turn (%)	Random (%)
	0	60.7	8.3	14.6	16.4
1	5	45.1	13.3	16.1	25.5
	10	29.1	17.8	16.3	36.8
	20	19.5	22.8	15.3	42.4
	0	60.7	8.3	14.6	16.4
2	5	44.1	13.9	16.5	25.5
	10	35.7	14.4	14.5	35.4
	20	21.3	21.6	15.3	41.8

atoms (Fig. 1) were respectively LanL2DZ and 6-31G, implemented in Gaussian 09 [26]. The energy minimized platinum complexes and the simulated HSA protein were both imported to the Molegro Virtual Docker (MVD) [27] workspace, in order to carry out the protein-ligand docking.

Molecular docking simulation is able to predict the preferred orientation of ligand with respect to the protein, when bound to each other to form a stable complex. It also gives information on the protein's binding site chosen by the ligand. These facts, in turn may be employed to

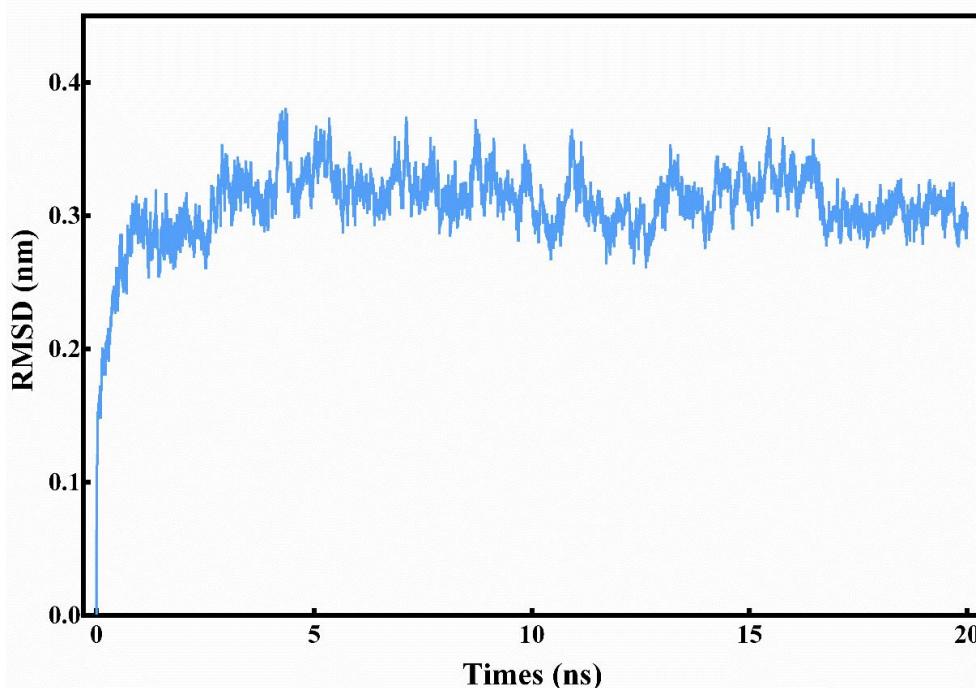


Fig. 9. The root mean square deviation (RMSD) of the HSA backbone vs. the initial 1BM0 chain A structure of HSA protein.

anticipate the strength of association or binding affinity between the bound molecules, using the scoring functions. The docking results, manifested in Fig. 10, reveal that complexes 1 and 2 prefer the binding sites I and II of the HSA molecule, respectively.

On the other hand, Table 6 reports the interaction energies of different amino acid residues of HSA molecule, with the two studied platinum complexes. The data indicates that Asp-183 and 187, Arg-186 and 428, Glu-425 and 520, Lys 519, Ile 523, Val 424 and Asn 429 interact effectively with the binuclear Pt(II) complex 1. In the case of the Pt complex 2, dominant interactions are with the amino acid residues of Arg160, Glu188 and 294, Asp 296, His 440, Lys 439 and 444 and Phe 156.

CONCLUSIONS

In this research, binding of binuclear platinum complexes (1 and 2) and HSA molecule was investigated through various spectroscopic techniques, and

thermodynamic parameters were used to determine the nature of dominant interactions. The molecular dynamics and docking simulations were also employed to specify the binding sites of these complexes on the HSA molecule and the amino acids contributing to the protein-ligand interactions. Overall results confirmed that the spontaneous enthalpy driven interaction of platinum complexes with HSA occurs through static and dynamic quenching mechanisms in complexes 1 and 2, respectively.

Moreover, analysis of the spectroscopic and binding thermodynamic parameters confirmed the structural changes of HSA, due to binding to the binuclear platinum complexes, and the main contributions to the interactions of HSA and platinum complexes were found to be the hydrogen bonding and van der Waals interactions.

Molecular docking results revealed binding of two studied platinum complexes to the different binding sites of HSA molecule, along with the interaction energies for all protein-ligand interactions. As a result of binding to platinum complexes, the α -helical content of HSA was

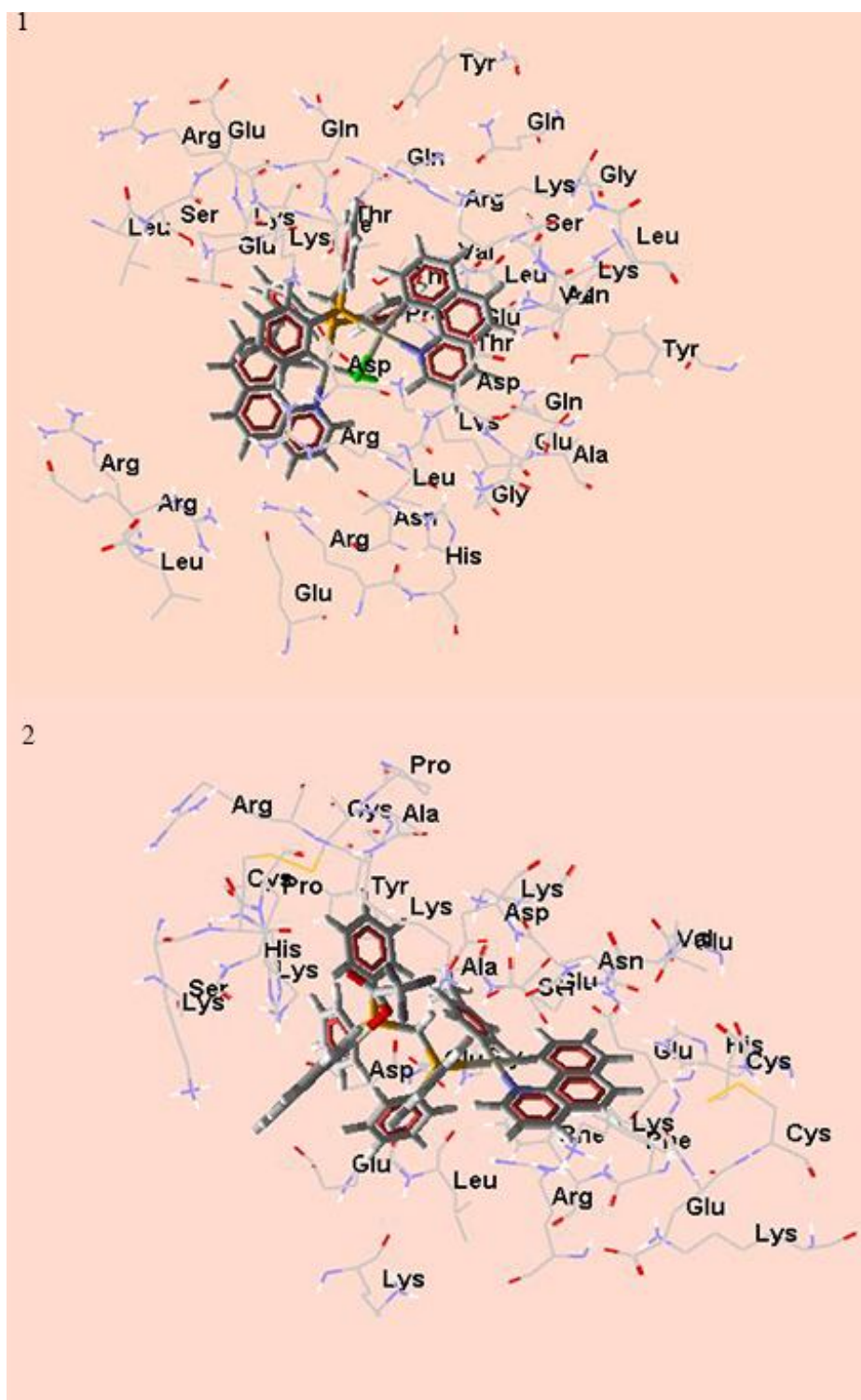


Fig. 10. The docking simulation analysis of the interaction between protein and synthetic binuclear platinum complexes.

Table 6. Interaction Energies of Amino Acid Residues of HSA in Binding with Binuclear Platinum Complexes (1 and 2) Obtained from Molecular Docking Analysis

Complex 1		Complex 2	
Amino acid residues	Interaction energies (kJ mol ⁻¹)	Amino acid residues	Interaction energies (kJ mol ⁻¹)
Arg-117	-0.60585	Phe-156	-8.46039
Glu-141	-1.26445	Phe-157	-0.4943
Arg-145	-0.30546	Arg-160	-12.8725
Asp-183	-12.8955	Glu-184	-2.9313
Arg-186	-20.4895	Asp-187	-0.6628
Asp-186	-10.0182	Glu-188	-23.5296
Glu-188	-0.77327	Ala-191	-0.47994
Lys	0.664676	Lys-195	-0.72886
Ala-191	-0.44987	Lys-276	-1.70135
Pro-421	-3.25761	His-288	-1.96953
Val-424	-6.27185	Cys-289	-2.37779
Glu-425	-19.3833	Glu-292	-1.39856
Arg-428	-14.5388	Glu-294	-22.2969
Asn-429	-7.74982	Asn-295	-1.11648
Lys-432	-0.95845	Asp-296	-5.76193
Lys-436	-2.93664	Ser-435	-2.49725
Tyr-452	-1.02715	Lys-436	-11.0041
Gln-459	-0.62881	Cys-437	-1.2989
Ser-517	-0.40466	Lys-439	-5.20078
Glu-518	-0.94765	His-440	-30.2457
Lys-519	-24.5091	Pro-441	-2.10935
Glu-520	-15.7473	Lys-444	-23.5054
Arg-521	-0.39247	Arg-445	-0.68692
Gln-522	-0.86635	Cys-448	-2.47498
Ile-523	-22.3699	Tyr-452	-0.38651
Lys-524	-4.30603		

reduced, while other protein's secondary structural features showed enhancements.

REFERENCES

- [1] Wong, E.; Giandomenico, C. M., Current status of platinum-based antitumor drugs. *Chem. Rev.* **1999**, *99*, 2451-2466, DOI: 10.1021/cr980420v.
- [2] Gao, E. J.; Wang, L.; Zhu, M. C.; Liu, L.; Zhang, W. Z., Synthesis, characterization, interaction with DNA and cytotoxicity *in vitro* of the complexes [M(dmphen)(CO₃)]·H₂O [M = Pt(II), Pd(II)]. *Eur. J. Med. Chem.* **2010**, *45*, 311-316, DOI: 10.1016/j.ejmech.2009.10.014.
- [3] Reedijk, J., Metal-ligand exchange kinetics in platinum and ruthenium complexes. *Platin. Met. Rev.* **2008**, *52*, 2-11, DOI: 10.1595/147106708x255987.
- [4] Dockal, M.; Carter, D. C.; Rüker, F., The three recombinant domains of human serum albumin. Structural characterization and ligand binding properties. *J. Biol. Chem.* **1999**, *274*, 29303-29310, DOI: 10.1074/jbc.274.41.29303.
- [5] Li, Y.; He, W. Y.; Liu, H.; Yao, X.; Hu, Z. Daidzein interaction with human serum albumin studied using optical spectroscopy and molecular modeling methods. *J. Mol. Struct.* **2007**, *831*, 144, DOI: 10.1016/j.molstruc.2006.07.034.
- [6] Fanali, G.; di Masi, A.; Trezza, V.; Marino, M.; Fasano, M.; Ascenzi, P., Human serum albumin: from bench to bedside. *Mol Aspects Med.* **2012**, *33*, 209-290, DOI: 10.1016/j.mam.2011.12.002.
- [7] Chaves, O. A.; Acunha, T. V.; Iglesias, B. A.; Jesus, C. S. H.; Serpa, C., Effect of peripheral platinum(II) bipyridyl complexes on the interaction of tetracationic porphyrins with human serum albumin. *J. Mol. Liq.* **2020**, *301*, 112466. DOI: 10.1016/j.molliq.2020.112466.
- [8] Shahabadi, N.; Amiri, S.; Taherpour, A., Human serum albumin binding studies of a new platinum(IV) complex containing the drug pregabalin: Experimental and computational methods. *J. Coord. Chem.* **2019**, *72*, 600-618. DOI: 10.1080/00958972.2019.1568419.
- [9] Yasrebi, S. A.; Takjoo, R.; Riazi, G. H., HSA-interaction studies of uranyl complexes of alkyl substituted isothiosemicarbazone. *J. Mol. Struct.* **2019**, *1193*, 53-61. DOI: 10.1016/j.molstruc.2019.04.126.
- [10] Hu, W.; Luo, Q.; Wu, K.; Li, X.; Wang, F.; Chen, Y.; Ma, X.; Wang, J.; Liu, J.; Xiong, S.; Sadler, P. J., The anticancer drug cisplatin can cross-link the interdomain zinc site on human albumin. *Chem. Commun.* **2011**, *47*, 6006-6008, DOI: 10.1039/c1cc11627d.
- [11] Shahsavani, M. B.; Ahmadi, S.; DadkhahAseman, M.; Nabavizadeh, S. M.; Alavianmehr, M. M.; Yousefi, R., Comparative study on the interaction of two binuclear Pt(II) complexes with human serum albumin: Spectroscopic and docking simulation assessments. *J. Photochem. Photobiol. B.* **2016**, *164*, 323-334, DOI: 10.1016/j.jphotobiol.2016.09.035.
- [12] Barzegar-Kiadehi, S. R.; GolbonHaghighi, M.; Jamshidi, M.; Notash, B., Influence of the diphosphine coordination mode on the structural and optical properties of cyclometalated platinum(II) complexes: An experimental and theoretical study on intramolecular Pt··Pt and $\pi\cdots\pi$ Interactions, *Inorg. Chem.* **2018**, *57*, 5060-5073, DOI: 10.1021/acs.inorgchem.8b00137.
- [13] SamandarSangari, M.; GolbonHaghighi, M.; Nabavizadeh, M.; Kubicki, M.; Rashidi, M., Photophysical study on unsymmetrical binuclear cycloplatinated(II) complexes. *New J. Chem.* **2017**, *41*, 13293-13302. DOI: 10.1039/C7NJ03034G.
- [14] Lakowicz, J. R., Principles of Fluorescence Spectroscopy, Springer, **2006**.
- [15] Muller, N.; Lopicque, F.; Drelon, E.; Netter, P., Binding sites of fluorescent probes on human serum albumin. *J. Pharm. Pharmacol.* **1994**, *46*, 300-304. DOI: 10.1111/j.2042-7158.1994.tb03798.x.
- [16] He, X. M.; Carter, D. C., Atomic structure and chemistry of human serum albumin. *Nature.* **1992**, *358*, 209-215, DOI: 10.1038/358209a0.
- [17] Cardamone M.; Puri N. K., Spectrofluorometric assessment of the surface hydrophobicity of proteins. *Biochem J.* **1992**, *282*, 589-593, DOI: 10.1042/bj2820589.
- [18] Zsila, F., Circular dichroism spectroscopic detection of ligand binding induced subdomain IB specific

- structural adjustment of human serum albumin. *J. Phys. Chem. B* **2013**, *117*, 10798-10806, DOI: 10.1021/jp4067108. 34.
- [19] Divsalar, A.; Saboury, A. A.; Yousefi, R.; Moosavi-Movahedi, A. A.; Mansoori-Torshizi, H., Spectroscopic and cytotoxic studies of the novel designed palladium(II) complexes: β -lactoglobulin and K562 as the targets, *Int. J. Biol. Macromol.* **2007**, *40*, 381-386, DOI: 10.1016/j.ijbiomac.2006.09.015.
- [20] Sugio, S.; Kashima, A.; Mochizuki, S.; Noda, M.; Kobayashi, K., Crystal structure of human serum albumin at 2.5 Å resolution. *Protein Eng.* **1999**, *12*, 439-446, DOI: 10.1093/protein/12.6.439.
- [21] Berendsen, H. J. C.; Van der Spoel, D.; van Drunen, R., GROMACS: A message-passing parallel molecular dynamics implementation. *Comput. Phys. Commun.* **1995**, *91*, 43-56, DOI: 10.1016/0010-4655(95)00042-E.
- [22] Hess B.; Kutzner, C.; Van der Spoel, D.; Lindahl, E., GROMACS 4: Algorithms for highly efficient, load-balanced, and scalable molecular simulation. *J. Chem. Theory. Comput.* **2008**, *4*, 435-447, DOI: 10.1021/ct700301q.
- [23] van Gunsteren, W. F.; Billeter, S. R.; Eising, A. A.; Hüenberger, P. H.; Krüger, P.; Mark, A. E.; Scott, W.; Tironi, W. R. P., Biomolecular Simulation: The GROMOS 96 Manual and User Guide; Swiss Federal Institute of Technology: Zurich, Switzerland, **1996**.
- [24] Oostenbrink, C.; Villa, A.; Mark, A. E.; van Gunsteren, W. F., A biomolecular force field based on the free enthalpy of hydration and solvation: The GROMOS force-field parameter sets 53A5 and 53A6. *J. Comput. Chem.* **2004**, *25*, 1656-1676, DOI: 10.1002/jcc.20090.
- [25] Hirshman, S. P.; Whitson, J. C., Steepest-descent moment method for three-dimensional magnetohydrodynamic equilibria. *Phys. Fluids.* **1983**, *26*, 3553-3568, DOI: 10.1063/1.864116.
- [26] Frisch, M. J.; Trucks, G. W.; Schlegel, H. B.; Scuseria, G. E.; Robb, M. A.; Cheeseman, J. R.; Scalmani, G.; Barone, V.; Mennucci, B.; Petersson, G. A.; *et al.* Gaussian 09, Revision A.01, Gaussian, Inc., Wallingford CT, **2009**.
- [27] Thomsen, R.; Christensen, M. H., MolDock: A new technique for high-accuracy molecular docking, *J. Med. Chem.* **2006**, *49*, 3315-3321, DOI: 10.1021/jm051197e.
- [28] Bourassa, P.; Dubeau, S.; Maharvi, G. M.; Fauq, A. H.; Thomas, T.; Tajmir-Riahi, H., Binding of antitumor tamoxifen and its metabolites 4-hydroxytamoxifen and endoxifen to human serum albumin. *Biochimie.* **2011**, *93*, 1089-1101, DOI:10.1016/j.biochi.2011.03.006.
- [29] Schmid, F. X., Biological Macromolecules: UV-Vis Spectrophotometry, John Wiley & Sons, 2001.
- [30] Ambrosetti, R.; Bianchini, R.; Fisichella, S.; Fichera, M.; Zandomenighi, M., Resolution of the absorbance and CD spectra and formation constants of the complexes between human serum albumin and methyl orange. *Chem. Eur. J.* **1996**, *2*, 149-156, DOI: 10.1002/chem.19960020206.
- [31] Zhang, G.; Zhao, N.; Wang, L., Fluorescence spectrometric studies on the binding of puerarin to human serum albumin using warfarin, ibuprofen and digitoxin as site markers with the aid of chemometrics. *J. Lumin.* **2011**, *131*, 2716-2724, DOI: 10.1016/j.jlumin.2011.07.011.
- [32] Divsalar, A.; Bagheri, M. J.; Saboury, A. A.; Mansoori-Torshizi, H.; Amani, M., Investigation on the interaction of newly designed anticancer Pd(II) complexes with different aliphatic tails and human serum albumin. *J. Phys. Chem. B* **2009**, *113*, 14035-14042, DOI: 10.1021/jp904822n.
- [33] Petitpas, I.; Bhattacharya, A. A.; Twine, S.; East, M.; Curry, S., Crystal structure analysis of warfarin binding to human serum albumin: anatomy of drug site I, *J. Biol. Chem.* **2001**, *276*, 22804-22809, DOI: 10.1074/jbc.M100575200.
- [34] Ghuman, J.; Zunszain, P. A.; Petitpas, I.; Bhattacharya, A. A.; Otagiri, M.; Curry, S., Structural basis of the drug-binding specificity of human serum albumin. *J. Mol. Biol.* **2005**, *353*, 38-52, DOI: 10.1016/j.jmb.2005.07.075.
- [35] Zhao, X.; Liu R.; Chi Z.; Teng Y.; Qin P., New insights into the behavior of bovine serum albumin adsorbed onto carbon nanotubes: comprehensive spectroscopic studies. *J. Phys. Chem. B* **2010**, *114*, 5625-5631, DOI: 10.1021/jp100903x.

- [36] Ross, P. D.; Subramanian, S., Thermodynamics of protein association reactions: forces contributing to stability. *Biochemistry*. **1981**, *20*, 3096-3102, DOI: 10.1021/bi00514a017.
- [37] Tang, J.; Lian, N.; He, X.; Zhang, G., Investigation of the interaction between sophoricoside and human serum albumin by optical spectroscopy and molecular modeling methods, *J. Mol. Struct.* **2008**, *889*, 408-414, DOI: 10.1016/j.molstruc.2008.02.031.
- [38] Lehrer, S. S., Solute perturbation of protein fluorescence. Quenching of the tryptophyl fluorescence of model compounds and of lysozyme by iodide ion. *Biochemistry*. **1971**, *10*, 3254, DOI: 10.1021/bi00793a015.
- [39] Möller, M.; Denicola, A., Study of protein-ligand binding by fluorescence. *Biochem. Mol. Biol. Educ.* **2002**, *30*, 309-312, DOI: 10.1002/bmb.2002.494030050089.
- [40] Ouameur, A. A.; Marty, R.; Tajmir-Riahi, H., Human serum albumin complexes with chlorophyll and chlorophyllin. *Biopolymers*. **2005**, *77*, 129-136, DOI: 10.1002/bip.20173.
- [41] Zhang, G.; Ma, Y., Mechanistic and conformational studies on the interaction of food dye amaranth with human serum albumin by multi spectroscopic methods, *Food Chem.* **2013**, *136* 442-449, DOI: 10.1016/j.foodchem.2012.09.026.
- [42] Hu, Y. J.; Li, W.; Liu, Y.; Dong, J. X.; Qu, S. S., Fluorometric investigation of the interaction between methylene blue and human serum albumin. *J. Pharm. Biomed. Anal.* **2005**, *39*, 740, DOI: 10.1016/j.jpba.2005.04.009.